J|A|C|S
ARTICLES
Published on Web 05/13/2006

Controlling Structure from the Bottom-Up: Structural and Optical Properties of Layer-by-Layer Assembled Palladium Coordination-Based Multilayers

Marc Altman,[†] Atindra D. Shukla,[†] Tatiana Zubkov,[†] Guennadi Evmenenko,[‡] Pulak Dutta,[‡] and Milko E. van der Boom*,[†]

Contribution from the Department of Organic Chemistry, The Weizmann Institute of Science, Rehovot, 76100, Israel, and Department of Physics and Astronomy, and the Materials Research Center, Northwestern University, Evanston, Illinois 60208-3113

Received February 22, 2006; E-mail: milko.vanderboom@weizmann.ac.il

Abstract: Layer-by-layer assembly of two palladium coordination-based multilayers on silicon and glass substrates is presented. The new assemblies consist of rigid-rod chromophores connected by terminal pyridine moieties to palladium centers. Both colloidal palladium and $PdCl_2(PhCN)_2$ were used in order to determine the effect of the metal complex precursor on multilayer structure and optical properties. The multilayers were formed by an iterative wet-chemical deposition process at room temperature in air on a siloxane-based template layer. Twelve consecutive deposition steps have been demostrated resulting in structurally regular assemblies with an equal amount of chromophore and palladium added in each molecular bilayer. The optical intensity characteristics of the metal−organic films are clearly a function of the palladium precursor employed. The colloid-based system has a UV−vis absorption maximum an order of magnitude stronger than that of the $PdCl_2$-based multilayer. The absorption maximum of the $PdCl_2$-based film exhibits a significant red shift of 23 nm with the addition of 12 layers. Remarkably, the structure and physiochemical properties of the submicron scale $PdCl_2$-based structures are determined by the configuration of the ~15 Å thick template layer. The refractive index of the $PdCl_2$-based film was determined by spectroscopic ellipsometry. Well-defined three-dimensional structures, with a dimension of 5 μm, were obtained using photopatterned template monolayers. The properties and microstructure of the films were studied by UV−vis spectroscopy, spectroscopic ellipsometry, atomic force microscopy (AFM), X-ray reflectivity (XRR), scanning electron microscopy (SEM), and aqueous contact angle measurements (CA).

Introduction

The stepwise assembly of organized arrays of molecules covalently bound to substrate surfaces offers an attractive, versatile method to design and construct a wide range of thin films with precise control over structure and material properties.[1−7] For instance, molecular layer-by-layer multilayer formation can result in the formation of intrinsically acentric materials with excellent electro-optical properties.[1,8−17] Of particular interest is the formation of hybrid organic−inorganic materials in which it is possible to control material function and properties by the nature and periodic table positions of the incorporated metal ions, colloids, and/or metal oxides.[14,15,18−27] Seminal work on

[†] The Weizmann Institute of Science.
[‡] Northwestern University.

(1) Li, D.; Ratner, M. A.; Marks, T. J.; Zhang, C.; Yang, J.; Wong, G. K. *J. Am. Chem. Soc.* **1990**, *112*, 7389−7390.
(2) Evans, S. D.; Urankar, E.; Ulman, A.; Ferris, N. *J. Am. Chem. Soc.* **1991**, *113*, 4121−4131.
(3) Ulman, A. *Chem. Rev.* **1996**, *96*, 1533−1554.
(4) Mallouk, T. E.; Kim, H.-N.; Ollivier, P. J.; Keller, S. W. *Compr. Supramol. Chem.* **1996**, *7*, 189−217.
(5) Naaman, R.; Vager, Z. *Acc. Chem. Res.* **2003**, *36*, 291−299.
(6) Salomon, A.; Cahen, D.; Lindsay, S.; Tomfohr, J.; Engelkes, V. B.; Frisbie, C. D. *Adv. Mater.* **2003**, *15*, 1881−1890.
(7) Ray, S. G.; Cohen, H.; Naaman, R.; Liu, H.; Waldeck, D. H. *J. Phys. Chem. B* **2005**, *109*, 14064−14073.
(8) Katz, H. E.; Scheller, G.; Putvinski, T. M.; Schilling, M. L.; Wilson, W. L.; Chidsey, C. E. D. *Science* **1991**, *254*, 1485−1487.
(9) Marks, T. J.; Ratner, M. A. *Angew. Chem., Int. Ed. Engl.* **1995**, *34*, 155−173.
(10) Bell, C. M.; Yang, H. C.; Mallouk, T. E. *Adv. Chem. Ser.* **1995**, *245*, 211−230.
(11) Hanken, D. G.; Naujok, R. R.; Gray, J. M.; Corn, R. M. *Anal. Chem.* **1997**, *69*, 240−248.
(12) Flory, W. C.; Mehrens, S. M.; Blanchard, G. J. *J. Am. Chem. Soc.* **2000**, *122*, 7976−7985.
(13) Neff, G. A.; Helfrich, M. R.; Clifton, M. C.; Page, C. J. *Chem. Mater.* **2000**, *12*, 2363−2371.
(14) van der Boom, M. E.; Evmenenko, G.; Dutta, P.; Marks, T. J. *Adv. Funct. Mater.* **2001**, *11*, 393−397.
(15) van der Boom, M. E.; Marks, T. J. Layer-by-Layer Assembly of Molecular Materials for Electrooptic Switching. In *Polymers for Micro- and Nano-Electronics*; Lin, Q., Hedrick, J. C., Pearson, R. A., Eds.; ACS Symposium Series 874; American Chemical Society: Washington, DC, 2004; pp 30−43.
(16) Rashid, A. N.; Gunter, P. *Org. Electron.* **2004**, *5*, 147−155.
(17) Zhao, Y. G.; Chang, S.; Wu, A.; Lu, H. L.; Ho, S. T.; van der Boom, M. E.; Marks, T. J. *Opt. Eng.* **2003**, *42*, 298−299.
(18) Lee, H.; Kepley, L. J.; Hong, H. G.; Mallouk, T. E. *J. Am. Chem. Soc.* **1988**, *110*, 618−620.
(19) Hatzor, A.; Moav, T.; Cohen, H.; Matlis, S.; Libman, J.; Vaskevich, A.; Shanzer, A.; Rubinstein, I. *J. Am. Chem. Soc.* **1998**, *120*, 13469−13477.
(20) Tillman, N.; Ulman, A.; Penner, T. L. *Langmuir* **1989**, *5*, 101−111.
(21) Kim, H.-N.; Keller, S. W.; Mallouk, T. E.; Schmitt, J.; Decher, G. *Chem. Mater.* **1997**, *9*, 1414−1421.
(22) Katz, H. E.; Schilling, M. L.; Ungashe, S.; Putvinski, T. M.; Chidsey, C. E. Synthesis and Deposition of Electronic Donors, Acceptors, and Insulators as Components of Zirconium Diphosphonate Multilayer Films. ACS Symposium Series 499; American Chemical Society: Washington, DC, 1992; pp 24−32.

 10.1021/ja061026e CCC: $33.50

siloxane-based monolayers and multilayer assemblies was carried out by Sagiv and others.[1,3,20,28−34] Mallouk and coworkers introduced layer-by-layer self-assembled metal−organic films, with organic modules linked by zirconium phosphate−phosphonate interlayers.[18,21,35−37] Coordination-based multilayers involving mainly zirconium group metals and various ligands have been reported, including composite multilayers with alternating linkers.[8,18,19,21,26,33,35,38−48] Numerous multilayered metal−organic assemblies have been studied in detail; however, the use of the platinum group metals is relatively rare.[23,24,49−52] The well-documented coordination chemistry of these metals in solution[53−55] might be utilized to form and control thin film structure and properties at the molecular level. Recently, Qian et al. reported the assembly of various palladium−porphyrin arrays bound to silicon and related substrates.[23−25] Colloid- or nanoparticles-based multilayer assemblies are also uncommon.[56−60] Device-quality organic assemblies have been integrated into prototype frequency-doubling devices, electro-optical modulators, and light-emitting diodes (OLEDs).[1,14,15,61−64] Multilayer assemblies are often difficult to pattern,[17,65] which is a necessary requirement for device formation. Therefore, there is much current interest in the development of "bottom-up" film growth methods. For example, Whitesides and others used microcontact printing and nanoprinting on various substrates to construct patterned organic mono- and multilayer films.[1,66−71] Here we report on solution-based layer-by-layer formation of palladium−organic assemblies. In this study, we compare the effect of the nature of the employed palladium precursors (i.e., colloids vs $PdCl_2$) on multilayer structure and optical properties. A rigid-rod chromophore having two pyridine units is used as the organic building block, allowing the film structure to be monitored by optical (UV−vis) spectroscopy in transmission mode. The pyridine moieties allow facile coordination to the palladium centers. We describe the relationship between the orientation of the template layer at the molecular level and its long-range retention in the $PdCl_2$-based multilayer film, which has important consequences for the design of this class of supramolecular assemblies. Furthermore, we report on the refractive index of the material formed and on the bottom-up three-dimensional (3D) assembly of a multilayer on a photopatterned monolayer.

Results and Discussion

Synthesis of Chromophore 2 and Template Layer Formation. Reaction of 1,4-bis[2-(4-pyridyl)ethenyl]benzene (**1**) with an excess of 3-iodo-*n*-propyl-1-trimethoxysilane in dry THF at elevated temperatures results in the quantitative formation of the corresponding pyridinium salt (eq 1). The reported methyl−pyridinium analogue has similar spectroscopic features.[72]

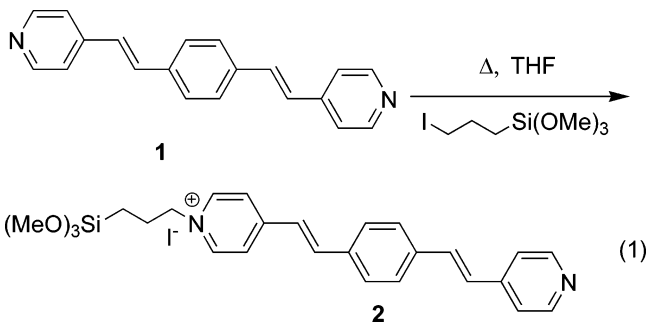

(1)

For instance, the ^1H NMR spectrum exhibits a characteristic triplet resonance at $\delta = 4.59$ ppm for the pyr−CH_2− moiety,[73,74] and the optical spectrum of **2** in acetone exhibits a typical red shift of 38 nm to $\lambda_{max} = 381$ nm in the charge-transfer band relative to compound **1** (Figure 1). Compound **2** was used for

(23) Qian, D.-J.; Nakamura, C.; Miyake, J. *Chem. Commun.* **2001**, 2312−2313.
(24) Qian, D.-J.; Nakamura, C.; Ishida, T.; Wenk, S.-O.; Wakayama, T.; Takeda, S.; Miyake, J. *Langmuir* **2002**, *18*, 10237−10242.
(25) Qian, D.-J.; Wakayama, T.; Nakamura, C.; Miyake, J. *J. Phys. Chem. B* **2003**, *107*, 3333−3335.
(26) Doron-Mor, I.; Cohen, H.; Cohen, S. R.; Popovitz-Biro, R.; Shanzer, A.; Vaskevich, A.; Rubinstein, I. *Langmuir* **2004**, *20*, 10727−10733.
(27) Libera, J. A.; Gurney, R. W.; Schwartz, C.; Jin, H.; Lee, T. L.; Nguyen, S. T.; Hupp, J. T.; Bedzyk, M. J. *J. Phys. Chem. B* **2005**, *109*, 1441−1450.
(28) Netzer, L.; Sagiv, J. *J. Am. Chem. Soc.* **1983**, *105*, 674−676.
(29) Li, D.; Swanson, B. I.; Robinson, J. M.; Hoffbauer, M. A. *J. Am. Chem. Soc.* **1993**, *115*, 6975−6980.
(30) Pomerantz, M.; Segmuller, A.; Netzer, L.; Sagiv, J. *Thin Solid Films* **1985**, *132*, 153−162.
(31) Ulman, A.; Tillman, N. *Langmuir* **1989**, *5*, 1418−1420.
(32) Durfor, C. N.; Turner, D. C.; Georger, J. H.; Peek, B. M.; Stenger, D. A. *Langmuir* **1994**, *10*, 148−152.
(33) Maoz, R.; Sagiv, J. *Adv. Mater.* **1998**, *10*, 580−584.
(34) Baptiste, A.; Gibaud, A.; Bardeau, J. F.; Wen, K.; Maoz, R.; Sagiv, J.; Ocko, B. M. *Langmuir* **2002**, *18*, 3916−3922.
(35) Lee, H.; Kepley, L. J.; Hong, H. G.; Akhter, S.; Mallouk, T. E. *J. Phys. Chem.* **1988**, *92*, 2597−2601.
(36) Hong, H. G.; Sackett, D. D.; Mallouk, T. E. *Chem. Mater.* **1991**, *3*, 521−527.
(37) Yang, H. C.; Aoki, K.; Hong, H. G.; Sackett, D. D.; Arendt, M. F.; Yau, S. L.; Bell, C. M.; Mallouk, T. E. *J. Am. Chem. Soc.* **1993**, *115*, 11855−11862.
(38) Byrd, H.; Whipps, S.; Pike, J. K.; Ma, J. F.; Nagler, S. E.; Talham, D. R. *J. Am. Chem. Soc.* **1994**, *116*, 295−301.
(39) Cassagneau, T.; Mallouk, T. E.; Fendler, J. H. *J. Am. Chem. Soc.* **1998**, *120*, 7848−7859.
(40) Frey, B. L.; Hanken, D. G.; Corn, R. M. *Langmuir* **1993**, *9*, 1815−1820.
(41) Hatzor, A.; van der Boom-Moav, T.; Yochelis, S.; Vaskevich, A.; Shanzer, A.; Rubinstein, I. *Langmuir* **2000**, *16*, 4420−4423.
(42) Kaschak, D. M.; Johnson, S. A.; Waraksa, C. C.; Pogue, J.; Mallouk, T. E. *Coordin. Chem. Rev.* **1999**, *185*−*186*, 403−416.
(43) Kaschak, D. M.; Mallouk, T. E. *J. Am. Chem. Soc.* **1996**, *118*, 4222−4223.
(44) Zeppenfeld, A. C.; Fiddler, S. L.; Ham, W. K.; Klopfenstein, B. J.; Page, C. J. *J. Am. Chem. Soc.* **1994**, *116*, 9158−9165.
(45) Ansell, M. A.; Zeppenfeld, A. C.; Yoshimoto, K.; Cogan, E. B.; Page, C. J. *Chem. Mater.* **1996**, *8*, 591−594.
(46) Bharathi, S.; Nogami, M.; Ikeda, S. *Langmuir* **2001**, *17*, 7468−7471.
(47) Doron-Mor, H.; Hatzor, A.; Vaskevich, A.; van der Boom-Moav, T.; Shanzer, A.; Rubinstein, I.; Cohen, H. *Nature* **2000**, *406*, 382−385.
(48) Katz, H. E.; Wilson, W. L.; Scheller, G. *J. Am. Chem. Soc.* **1994**, *116*, 6636−6640.
(49) Bell, C. M.; Keller, S. W.; Lynch, V. M.; Mallouk, T. E. *Mater. Chem. Phys.* **1993**, *35*, 225−232.
(50) Offord, D. A.; Sachs, S. B.; Ennis, M. S.; Eberspacher, T. A.; Griffin, J. H.; Chidsey, C. E. D.; Collman, J. P. *J. Am. Chem. Soc.* **1998**, *120*, 4478−4487.
(51) Milic, T. N.; Chi, N.; Yablon, D. G.; Flynn, G. W.; Batteas, J. D.; Drain, C. M. *Angew. Chem., Int. Ed.* **2002**, *41*, 2117−2119.
(52) Milic, T.; Garno, J. C.; Batteas, J. D.; Smeureanu, G.; Drain, C. M. *Langmuir* **2004**, *20*, 3974−3983.
(53) Collman, J. P.; McDevitt, J. T.; Leidner, C. R.; Yee, G. T.; Torrance, J. B.; Little, W. A. *J. Am. Chem. Soc.* **1987**, *109*, 4606−4614.
(54) Collman, J. P.; Hegedus, L. S.; Norton, J. R.; Finke, R. G. *Principles and Applications of Organotransition Metal Chemistry*, 2nd ed.; University Science Books: Mill Valley, CA, 1987.
(55) Lehn, J. M. *Angew. Chem., Int. Ed. Engl.* **1988**, *27*, 89−112.
(56) Liu, J. Y.; Cheng, L.; Song, Y. H.; Liu, B. F.; Dong, S. J. *Langmuir* **2001**, *17*, 6747−6750.
(57) Liu, Y.; Wang, Y.; Claus, R. O. *Chem. Phys. Lett.* **1998**, *298*, 315−319.
(58) Lu, C.; Bai, S.; Zhang, D.; Huang, L.; Ma, J.; Luo, C.; Cao, W. *Nanotechnology* **2003**, *14*, 680−683.
(59) Supriya, L.; Claus, R. O. *J. Phys. Chem. B* **2005**, *109*, 3715−3718.
(60) Crespo-Biel, O.; Dordi, B.; Reinhoudt, D. N.; Huskens, J. *J. Am. Chem. Soc.* **2005**, *127*, 7594−7600.
(61) Facchetti, A.; Beverina, L.; van der Boom, M. E.; Dutta, P.; Evmenenko, G.; Shukla, A. D.; Stern, C. E.; Pagani, G. A.; Marks, T. J. *J. Am. Chem. Soc.* **2006**, *128*, 2142−2153.
(62) Lin, W.; Wong, G. K.; Marks, T. J. *J. Am. Chem. Soc.* **1996**, *118*, 8034−8042.
(63) Yerushalmi, R.; Scherz, A.; van der Boom, M. E.; Kraatz, H.-B. *J. Mater. Chem.* **2005**, *15*, 4480−4487.
(64) Yoon, M.-H.; Facchetti, A.; Marks, T. J. *Proc. Nat. Acad. Sci. U.S.A.* **2005**, *102*, 4678−4682.
(65) Zhao, Y.-G.; Wu, A.; Lu, H.-L.; Chang, S.; Lu, W.-K.; Ho, S. T.; van der Boom, M. E.; Marks, T. J. *Appl. Phys. Lett.* **2001**, *79*, 587.

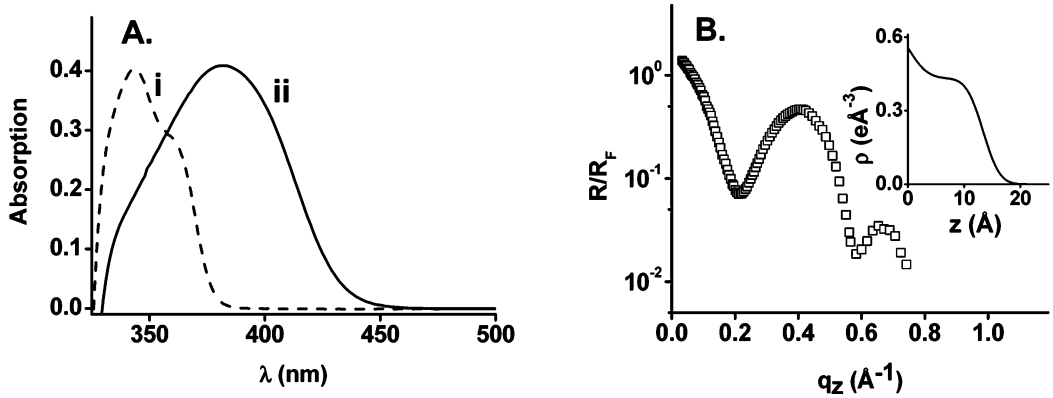

Figure 1. (A) Optical absorption (UV−vis) measurements of (i) compound **1** in acetone (0.01 mM) and (ii) compound **2** in acetone (0.01 mM) and (B) Synchrotron XRR data from a monolayer of compound **2**. Inset: Electron density profile of the monolayer film.

the formation of a pyridine terminated template layer. Freshly cleaned glass, ITO (indium−tin-oxide coated glass), and silicon were immersed in a dry THF solution of chromophore **2** (0.4 mM) and heated at 77 °C for 16 h in a sealed glass pressure vessel under N_2 with the exclusion of light. The functionalized silicon and the light-yellow colored glass substrates were thoroughly rinsed and sonicated repeatedly with copious amounts of organic solvents and were dried under a stream of N_2, followed by cleaning with a stream of critical CO_2.[75] The template layers formed adhere strongly to the various substrates and, when stored with the exclusion of light, were stable for months under otherwise ambient conditions, as judged by UV−vis spectroscopy. Neither washing with common organic solvents nor mechanical abrasion removed the films which were only compromised after prolonged exposure to concentrated HCl, as indicated by a decrease in UV−vis absorption. The new template layer was characterized by a variety of techniques, including UV−vis optical spectroscopy (UV−vis) and spectroscopic ellipsometry, semicontact atomic force microscopy (AFM), static contact angle (CA) measurements, X-ray photoelectron spectroscopy (XPS), and specular X-ray reflectivity (XRR). The fact that prolonged reaction times did not increase optical absorption indicates the formation of a fully formed film.[76] The average molecular density (≈2.2 molecules/nm^2) of the template layer of **2** was estimated from the optical data assuming that the molar extinction coefficient (ϵ) of the film is similar to that observed in solution ($\epsilon_{381} \approx 4.0 \times 10^4$ cm^{-1} M^{-1}).[32] This is in good agreement with previously reported density values of uniform stilbene-based monolayers.[74,76] In support of the optical data, semicontact mode AFM images of the functionalized silicon substrates show a relatively smooth film surface with no apparent features (e.g., islands, grains) or defects. Horizontal polymerization is known to result in the formation of relatively large features which would have been readily observable by AFM.[77−79] Root-mean-squared roughness (R_{rms}) measured for 500 nm × 500 nm scan areas are ∼0.4 nm (see the Supporting Information for details, Figure S1). The CA measurements show a moderately hydrophobic surface with $\theta = 72 \pm 5°$. XPS measurements of films formed on ITO showed the presence of the pyridinium nitrogen at 402.2 eV and the pyridine nitrogen at 399.8 eV.[80] The XPS-derived film thickness was estimated to be 12 ± 2 Å,[74] whereas the synchrotron XRR-determined thickness was 14.5 ± 0.5 Å, with a monolayer-air roughness of ∼2.4 Å. This shows that the chromophores are not standing straight-up perpendicular to the surface. The electron density (ρ), as determined by XRR, was 0.42 ± 0.02 eÅ^{-3}, indicating a densely packed film.[81,82] The XRR-determined average molecular density of ∼2.4 molecules/nm^2 is in good agreement with the aforementioned UV−vis data, which corresponds to a packing density of ∼1.7 molecules/nm^3 and further demonstrates a highly packed film structure.[74,81,82] The length of chromophore **2** (as estimated by the Chem3D Pro energy minimization model) is ∼21 Å. However, the perpendicular orientation of the alkyl-silane group on the surface and the highly slanted 3-ring portion of chromophore **2** result in a distance of ∼12 Å between the nitrogen atom of the terminal pyridine unit and the substrate. As a consequence, the upper portion of the chromophore is extended at an angle of only ∼20°, relative to the surface plane.

Stepwise Formation of Pd Colloid- and $PdCl_2$-Based Multilayers. The multilayer structure shown in Figure 2 was obtained by an iterative two-step all-wet chemical deposition method using identical template layers. Template layer func-

(66) Hatzor, A.; Weiss, P. S. *Science* **2001**, *291*, 1019−1020.
(67) Anderson, M. E.; Smith, R. K.; Donhauser, Z. J.; Hatzor, A.; Lewis, P. A.; Tan, L. P.; Tanaka, H.; Horn, M. W.; Weiss, P. S. *J. Vac. Sci. Technol., B* **2002**, *20*, 2739−2744.
(68) Huck, W. T. S.; Yan, L.; Stroock, A.; Haag, R.; Whitesides, G. M. *Langmuir* **1999**, *15*, 6862−6867.
(69) Tour, J. M.; Jones, L., II; Pearson, D. L.; Lamba, J. J. S.; Burgin, T. P.; Whitesides, G. M.; Allara, D. L.; Parikh, A. N.; Atre, S. *J. Am. Chem. Soc.* **1995**, *117*, 9529−9534.
(70) Sharpe, R. B. A.; Burdinski, D.; Huskens, J.; Zandvliet, H. J. W.; Reinhoudt, D. N.; Poelsema, B. *J. Am. Chem. Soc.* **2005**, *127*, 10344−10349.
(71) Bruinink, C. M.; Nijhuis, C. A.; Peter, M.; Dordi, B.; Crespo-Biel, O.; Auletta, T.; Mulder, A.; Schoenherr, H.; Vancso, G. J.; Huskens, J.; Reinhoudt, D. N. *Chem.−Eur. J.* **2005**, *11*, 3988−3996.
(72) Coe, B. J.; Jones, L. A.; Harris, J. A.; Brunschwig, B. S.; Asselberghs, I.; Clays, K.; Persoons, A.; Garin, J.; Orduna, J. *J. Am. Chem. Soc.* **2004**, *126*, 3880−3891.
(73) van der Boom, M. E.; Richter, A. G.; Malinsky, J. E.; Lee, P. A.; Armstrong, N. R.; Dutta, P.; Marks, T. J. *Chem. Mater.* **2001**, *13*, 15−17.
(74) Shukla, A. D.; Strawser, D.; Lucassen, A. C. B.; Freeman, D.; Cohen, H.; Jose, D. A.; Das, A.; Evmenenko, G.; Dutta, P.; van der Boom, M. E. *J. Phys. Chem. B* **2004**, *108*, 17505−17511.
(75) Chow, B. Y.; Mosley, D. W.; Jacobson, J. M. *Langmuir* **2005**, *21*, 4782−4785.
(76) van der Boom, M. E.; Evmenenko, G.; Yu, C.; Dutta, P.; Marks, T. J. *Langmuir* **2003**, *19*, 10531−10537.
(77) Bunker, B. C.; Carpick, R. W.; Assink, R. A.; Thomas, M. L.; Hankins, M. G.; Voigt, J. A.; Sipola, D.; de Boer, M. P.; Gulley, G. L. *Langmuir* **2000**, *16*, 7742−7751.
(78) Fadeev, A. Y.; McCarthy, T. J. *Langmuir* **2000**, *16*, 7268−7274.
(79) Moon, J. H.; Shin, J. W.; Kim, S. Y.; Park, J. W. *Langmuir* **1996**, *12*, 4621−4624.
(80) Yerushalmi, R.; Scherz, A.; van der Boom, M. E. *J. Am. Chem. Soc.* **2004**, *126*, 2700−2701.
(81) Gupta, T.; Altman, M.; Shukla, A. D.; Freeman, D.; Leitus, G.; van der Boom, M. E. *Chem. Mater.* **2006**, *18*, 1379−1382.
(82) Evmenenko, G.; van der Boom, M. E.; Kmetko, J.; Dugan, S. W.; Marks, T. J.; Dutta, P. *J. Chem. Phys.* **2001**, *115*, 6722−6727.

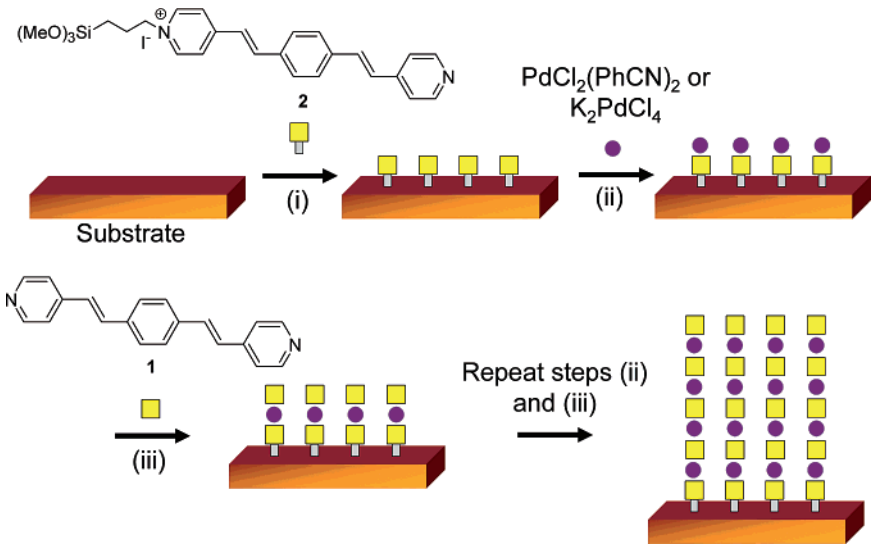

Figure 2. Schematic representation of the two-step layer-by-layer solution-based multilayer assembly. The same strategy was applied for the palladium-colloid-based system and the $PdCl_2$-based system. The multilayer formation can be conveniently carried out in air at room temperature.

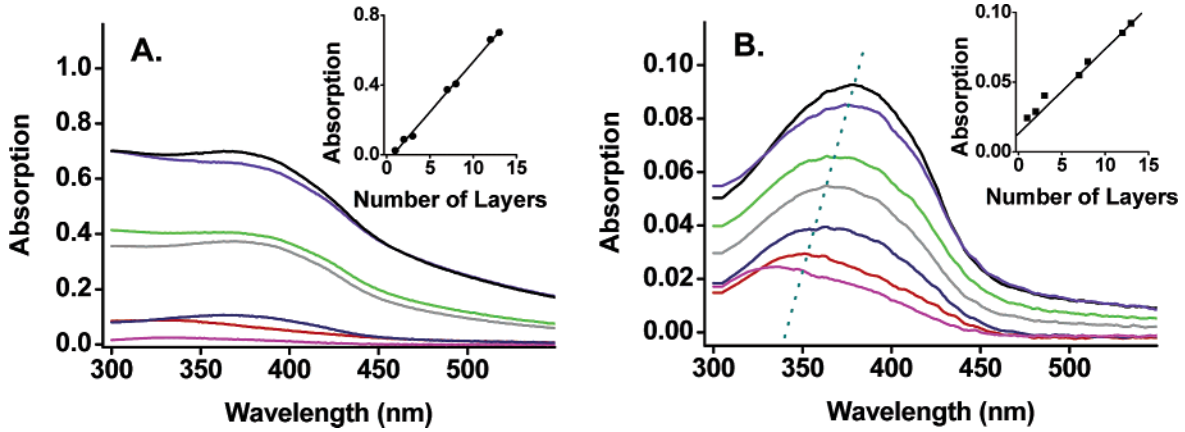

Figure 3. (A) UV−vis spectra for selected layers of a colloid-based assembly. No obvious shift in λ_{max} was observed. Inset: Optical absorption at $\lambda = 368$ nm for a colloid-based multilayer (●, $R^2 = 0.99$) for layers 1, 2, 3, 7, 8, 12, and 13 of a $PdCl_2$-based multilayer (□, $R^2 = 0.99$) and (B) UV−vis spectra for selected layers of a $PdCl_2$-based assembly showing a shift in λ_{max} from 337 to 379 nm for layers 1−13, including a linear fit of the 23 nm shift for layers 2−13 (dotted line, $R^2 = 0.90$). Inset: Optical absorption at λ_{max} nm for layers 1, 2, 3, 7, 8, 12, and 13 of a $PdCl_2$-based multilayer (■, $R^2 = 0.99$)

tionalized glass, ITO, and silicon substrates were immersed for 30 min in 0.3 mM K_2PdCl_4 in DI water at room temperature, then rinsed in DI water, and dried under a stream of N_2. Subsequently, the samples were immersed for another 30 min in a 1 mM solution of compound **1** in THF at room temperature, then sonicated in copious amounts of solvent, and dried under an N_2 stream. These two deposition steps were repeated 6 times each in air. To evaluate the effect of the metal complex precursor on the thin film structure and properties, and to demonstrate the scope and versatility of this deposition methodology, we employed the same deposition scheme used for the colloid-based multilayer to assemble multilayer films starting from chromophore **1** and $PdCl_2(PhCN)_2$. Template layer functionalized glass and silicon substrates were immersed for 15 min in a THF solution of $PdCl_2(PhCN)_2$ (1 mM), followed by 15 min in a THF solution of compound **1** (1 mM), and then rinsed in copious amounts of THF. These two steps were repeated 6 times each in air at room temperature. It is known that pyridine derivatives coordinate in solution in a mutually trans arrangement to $PdCl_2$.[51,52]

UV−vis measurements in transmission mode of the colloid-based system show a good linear correlation with $R^2 = 0.99$ between the optical absorption at $\lambda_{max} \approx 363$ nm and the number of chromophore layers (Figure 3A). This indicates the formation of a structurally regular multilayer with an equal density of chromophore **2** and palladium colloids deposited in each layer. After a shift in λ_{max} from 330 nm to ~363 nm between the template layer and the subsequent layers, no additional shift in the absorption maximum is observed. Likewise, UV−vis measurements of the $PdCl_2$-based assembly show a good linear correlation with $R^2 = 0.99$ between the absorption at λ_{max} and the number of chromophore layers, indicating that this deposition scheme also results in the formation of a microstructurally regular multilayer (Figure 3B). The constant increase in the optical absorption, $\Delta A \approx 0.012$, for each additional bilayer is slightly less than that of the monolayer. The colloid-based system has a UV−vis absorption maximum an order of magnitude stronger than that of the $PdCl_2$-based multilayer. A $PdCl_2$ unit can coordinate to two chromophore molecules in trans position,[52] whereas the colloid-based system had a more complex structure with a thick inorganic interlayer. Another remarkable difference between the two systems is a progressive bathochromic shift in the absorption maximum of the entire $PdCl_2$-based assembly with each additional layer from 337 nm

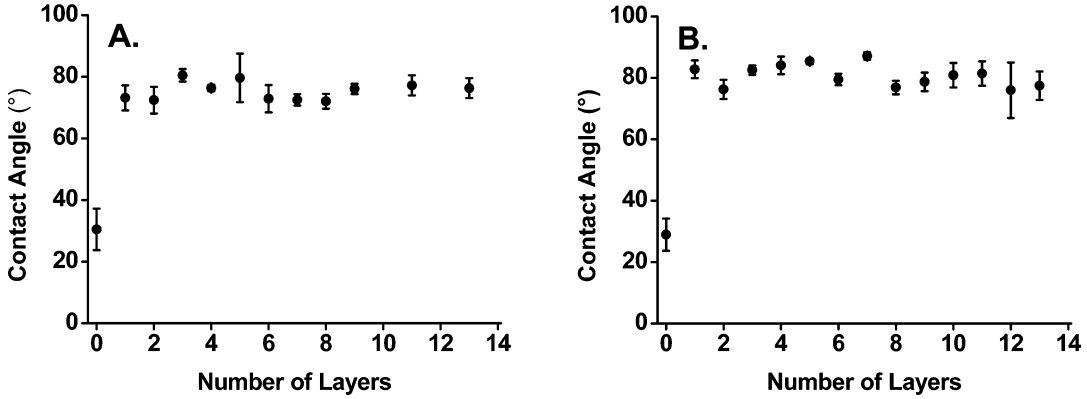

Figure 4. Static water contact angle vs number of layers of a (A) colloid-based multilayer and (B) $PdCl_2$-based multilayer with standard deviation error bars. Layer "0" indicates the contact angle of the bare silicon substrate.

for the template layer to 379 nm at layer 13, indicating electron communication between the topmost layer and the substrate and possible *J*-type aggregation.[74] The largest shift in λ_{max}, from 337 to 351 nm, occurred with the first $PdCl_2$ complexation to the template layer.

Static aqueous contact angle measurements did not reveal any difference between colloid and chromophore terminated layers. Likewise, there was no change in the contact angle with the addition of subsequent layers. The static contact angle for all layers, including the template layer, shown in Figure 4A, was $80 \pm 10°$, indicating the formation of a moderately hydrophilic structure. For each individual layer, however, the standard deviation was only $\pm 3°$. The exposed surface is not expected to vary with the addition of subsequent layers since both the AFM and XRR determined roughnesses of the films beyond the second layer are of the same order as the thickness of the film components. The static contact angle of the $PdCl_2$-based assembly is $75 \pm 5°$ for both the metal-complex- and chromophore-terminated layers (Figure 4B). This seems reasonable since the molecules are highly tilted relative to the surface normal (vide infra), resulting in a constant composition of the exposed surface from layer to layer.

Semicontact AFM imaging was carried out on multilayers formed on silicon substrates. The AFM-determined R_{rms} of the colloid-based multilayers, calculated over a 500 nm × 500 nm scan area, is 1.6−2.0 nm. This is consistent with the XRR determined roughness of 1.0−2.0 nm and is similar to or smoother than those of previously reported metal−organic multilayer assemblies.[19,24,26,56] No difference was noted between colloid-terminated and chromophore-terminated layers since most of the roughness is generated in the first colloid layer (layer 2). Representative semicontact AFM scans (Figure 5A, B) of a colloid-terminated 12-layered film and of the subsequent chromophore-terminated layer 13 both show comparable films with some apparent roughness. Semicontact AFM images of the $PdCl_2$-based system show smoother film surfaces, as compared to the colloid-based system. The R_{rms} calculated over a 500 nm × 500 nm scan area was <0.4 nm for both metal-complex-terminated and chromophore-terminated layers, an order of magnitude less than that of the colloid-based system.

The XRR thickness data, presented in Figure 6A and B, show clearly a linear increase in thickness with each additional bilayer for both systems. As shown in Figure 6A, each additional palladium colloid layer contributed on average to a 4.9 nm increase in thickness with $R^2 = 0.997$, while each chromophore layer had an average thickness of 0.73 nm with $R^2 = 0.994$. The large difference in thickness between the organic and the inorganic layers results in a "staircase" in the XRR thickness plot. The high thickness of the palladium interlayer may indicate that aggregation occurred either in the aqueous medium or on the surface. The XRR-derived electron density for all layers is $\rho \approx 0.4$ eÅ^{-3}. Figure 6E shows the Patterson function for the XRR data of layer 13. This Fourier transform representation of the data shows the distinct interface layers formed by the metal colloids.[83] For the $PdCl_2$-based system, the average bilayer thickness is only 0.4 nm ($R^2 = 0.99$, Figure 6B). This demonstrates that the molecules in the multilayer assembly are highly slanted, relative to the surface normal. This is a direct result of the distinct bent shape of chromophore **2** in the template layer[84] and of the well-defined Pd(II)−pyridine coordination chemistry.[52,54] The ∼110° angle between the alkyl-silane and 3-ring portions of chromophore **2** results in growth of subsequent layers at an angle of only ∼20° relative to the substrate. At that angle, the addition of each layer of chromophore **1**, with a length of ∼1.6 nm,[85] would result in an ∼0.5 nm increase in the thickness of the multilayer assembly. The experimental data confirm that the orientation of the entire assembly is determined by the ∼1.5 nm thick template layer. This shows that by choosing the appropriate template layer it is possible to control the properties of the entire multilayer assembly. This is especially important for assemblies consisting of molecules which have vastly different optical or chemical properties along their different axes.[61,80,86−88] The electron density is $\rho = 0.42 \pm 0.02$ eÅ^{-3} for all layers (Figure 6F), supporting the hypothesis of the formation of a homogeneous superlattice. The Patterson plot in Figure 6E shows no distinct interface layers in the $PdCl_2$-based films, in contrast to the colloid-based multilayer. This is likely because the dimensions of the former are below the detectable limit due to the structural characteristics of these films.

Spectroscopic ellipsometry was used to determine the real part of the refractive index $n(\lambda)$ of the assemblies by fitting the

(83) Evmenenko, G.; Dugan, S. W.; Kmetko, J.; Dutta, P. *Langmuir* **2001**, *17*, 4021−4024.
(84) Serbutoviez, C.; Nicoud, J.-F.; Fischer, J.; Ledoux, I.; Zyss, J. *Chem. Mater.* **1994**, *6*, 1358−1368.
(85) Lucassen, A. C. B.; Karton, A.; Leitus, G.; Shimon, L. J. W.; Martin, J. M. L.; van der Boom, M. E., submitted.
(86) van der Boom, T.; Hayes, R. T.; Zhao, Y.; Bushard, P. J.; Weiss, E. A.; Wasielewski, M. R. *J. Am. Chem. Soc.* **2002**, *124*, 9582−9590.
(87) Hoeben, F. J. M.; Jonkheijm, P.; Meijer, E. W.; Schenning, A. P. H. J. *Chem. Rev.* **2005**, *105*, 1491−1546.
(88) Kim, J.; Swager, T. M. *Nature* **2001**, *411*, 1030−1034.

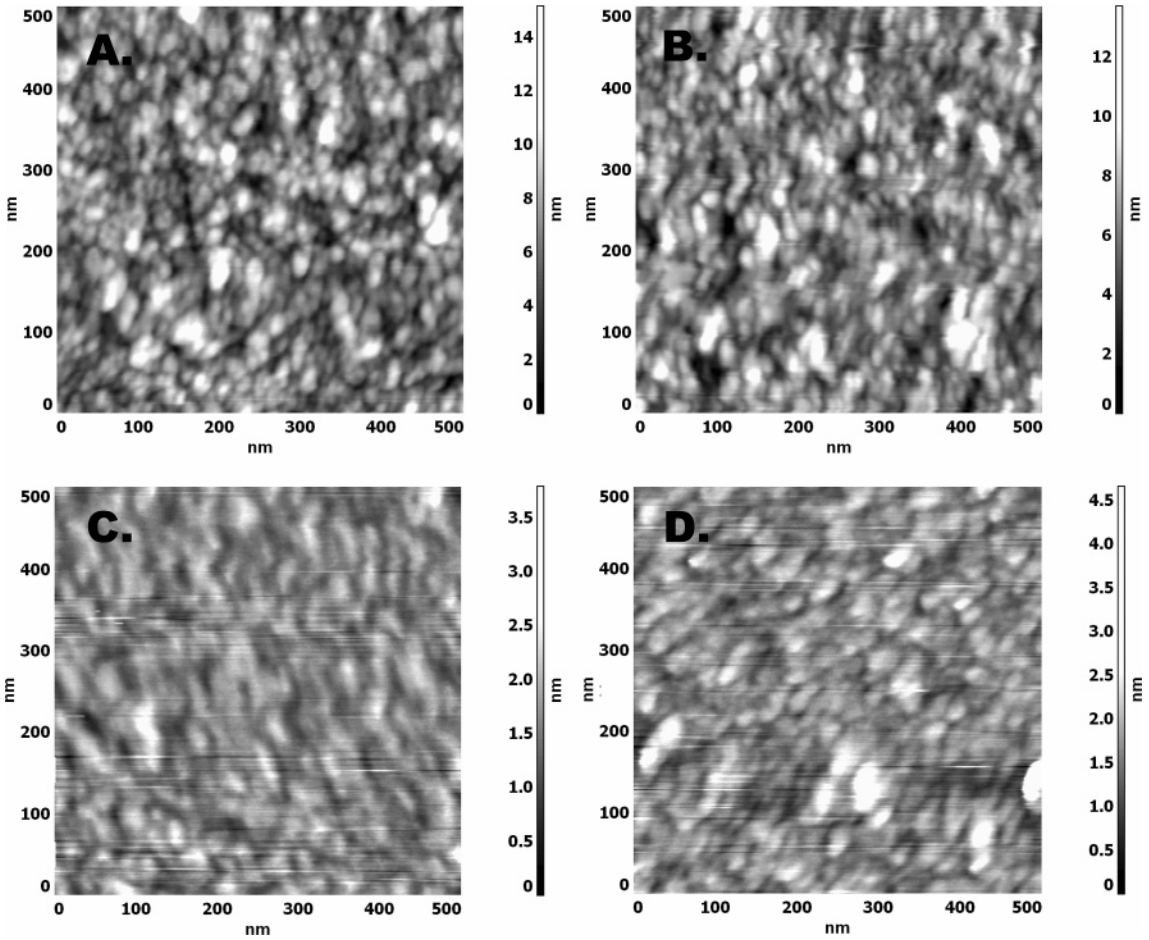

Figure 5. Representative semicontact AFM images at a 500 nm × 500 nm scan area of a (A) metal-terminated colloid-based multilayer (layer 12, R_{rms} = 2.0 nm), (B) chromophore-terminated colloid-based multilayer (layer 13, R_{rms} = 1.7 nm), (C) metal-terminated $PdCl_2$-based multilayer (layer 12, R_{rms} = 0.3 nm), and (D) chromophore-terminated $PdCl_2$-based multilayer (layer 13, R_{rms} = 0.4 nm).

three-term Cauchy equation to the XRR-determined film thickness in the nonabsorbing range of $\lambda = 600-1000$ nm (see the Supporting Information for details, Figure S2). The characterization of the optical constants of self-assembled multilayers by spectroscopic ellipsometry is rare,[61] though ellipsometry routinely has been used to determine the thickness of multilayer assemblies.[14,62] The refractive index n of the template layer is ~2.02 at $\lambda = 633$ nm. The high value of n relative to alkane-based monolayers[7,90,91] and other organic-based multilayers[18,65,89] is believed to reflect the relatively high conjugation of the chromophore **2** salt and is consistent with recent studies of highly conjugated monolayer films.[92] The thickness of the underlying oxide layer used in the model fit was 14 Å, which was also determined by XRR. The value of n decreased with the addition of subsequent layers, until a value of 1.98−1.99 was obtained for layers 5−13 (Figure 7). This phenomenon may be attributed to the increase in electron delocalization which becomes less significant with the addition of many layers. This "stabilization effect" of the refractive index can be compared with the stabilization of contact angle observed by Rubenstein and co-workers after a similar number of layers.[19,26] The refractive index of the colloid-based multilayer was not determined because of the complexity of fitting the data for rougher, less organized films. A summary of the main characteristics of both multilayers is provided in Table 1.

Bottom-Up Formation of 3D-Defined Pd-Colloid-Based Multilayers on Photopatterned Monolayers. Recently reported photopatterned films were used as a template layer for the bottom-up design of Pd-colloid-based multilayers.[93] Monolayers of trimethoxy-[11-(2-nitro-benzyloxy)-undecyl]-silane covalently bound to silicon and glass substrates were photoirradiated at $\lambda = 312 \pm 10$ nm through a chrome-plated mask with a 5 μm line and a pitch of 40 μm. This results in the selective removal of the photolabile 2-nitroso-benzaldehyde group in the exposed regions, leaving terminal, reactive hydroxyl moieties. The functionalized photopatterned substrates were immersed in an aqueous K_2PtCl_4, to bind the palladium selectively to the irradiated regions. This deposition step was followed by immersion of the substrates in a solution of compound **1**. UV−vis measurements on eight-layer assemblies grown on fully photodeprotected monolayers show identical absorption spectra as those for multilayers grown on the **2**-based template layer. Apparently, the nature of the template monolayer has little to

(89) Li, D.; Lutt, M.; Fitzsimmons, M. R.; Synowicki, R.; Hawley, M. E.; Brown, G. W. *J. Am. Chem. Soc.* **1998**, *120*, 8797−8804.
(90) Bordi, F.; Cametti, C.; Prato, M.; Cavalieri, O.; Canepa, M.; Gliozzi, A. *J. Phys. Chem. B* **2004**, *108*, 20263−20272.
(91) Stapleton, J. J.; Harder, P.; Daniel, T. A.; Reinard, M. D.; Yao, Y.; Price, D. W.; Tour, J. M.; Allara, D. L. *Langmuir* **2003**, *19*, 8245−8255.
(92) Marx, E.; Greenham, N. C.; Walzer, K.; Stokbro, K.; Less, R. J.; Raithby, P. R. *Org. Electron.* **2004**, *5*, 315−320.
(93) Zubkov, T.; Lucassen, A. C. B.; Freeman, D.; Feldman, Y.; Cohen, S. R.; Evmenenko, G.; Dutta, P.; van der Boom, M. E. *J. Phys. Chem. B* **2005**, *109*, 14144−14153.

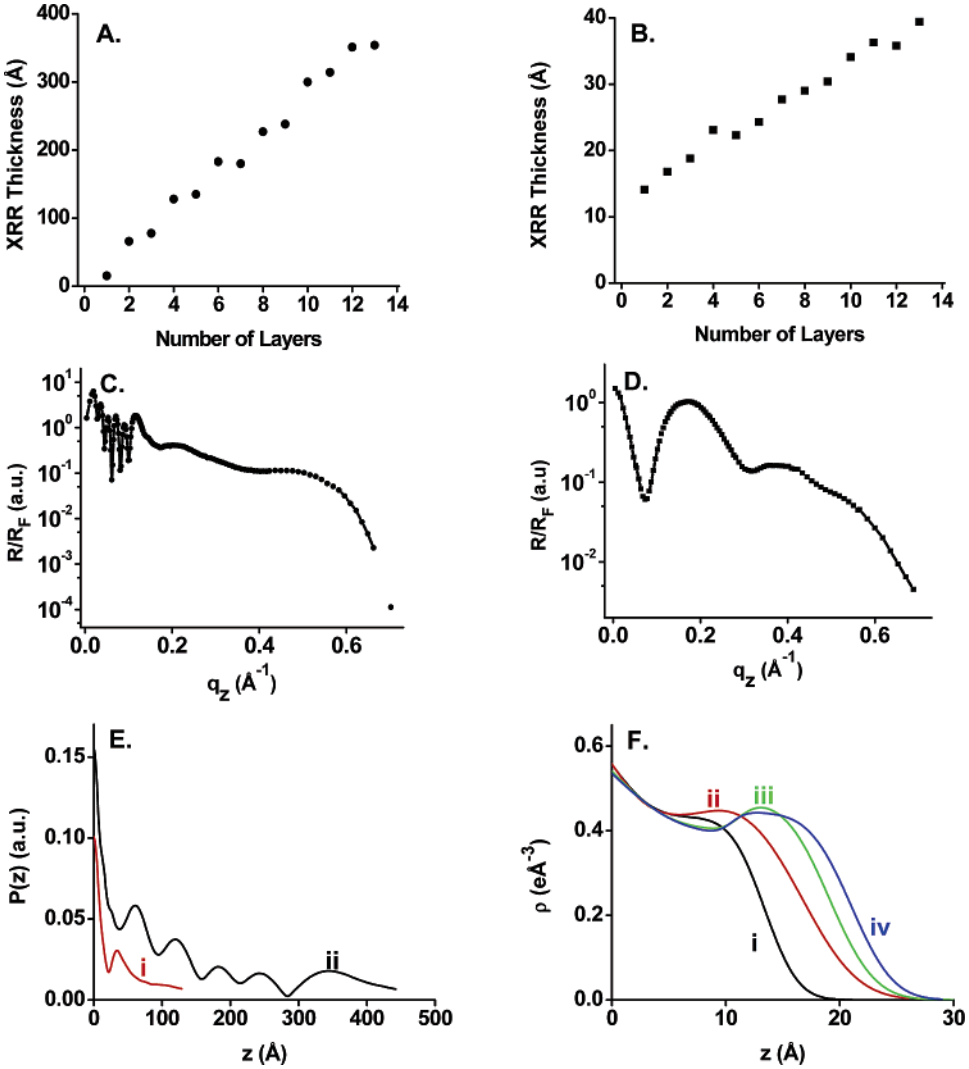

Figure 6. (A) XRR film thickness as a function of the number of layers for the colloid-based multilayer. (B) XRR film thickness as a function of the number of layers for the $PdCl_2$-based multilayer. (C) Representative XRR spectrum for layer 13 of the colloid-based multilayer. (D) Representative XRR spectrum for layer 13 of the $PdCl_2$-based multilayer. (E) Patterson plots of the XRR data for layer 13 of (i) the $PdCl_2$-based multilayer and (ii) the colloid-based multilayer. (F) Representative XRR electron density plots for $PdCl_2$-based multilayers for layers (i) 1, (ii) 2, (iii) 3, and (iv) 5. Corresponding plots for the colloid-based multilayer were not relevant due to interlayer and film roughness.

Table 1. Comparison of Main Properties of Colloid-Based and $PdCl_2$-Based Multilayer Assemblies

	avg bilayer thickness (nm)	typical AFM/XRR roughnes (nm)	UV–vis ΔA per bilayer	avg $\Delta\lambda_{max}$ between bilayers (nm)	refractive index n layer 13	aqueous contact angle layer 13 (deg)	λ_{max} layer 13 (nm)	XRR thickness layer 13 (nm)
colloid-based	5.6	1.7	0.11	0		76	367	354
$PdCl_2$-based	0.4	0.3	0.012	5	1.99	77	379	39.4

no effect on the optical features of the colloid-based assembly. No film growth was observed on protected monolayers. A scanning electron microscopy image of two bilayers grown on the patterned monolayers is shown in Figure 8. The areas coated with the more conductive metal-colloid terminated multilayers appear as dark and distinct lines relative to the bare template layer.

Summary and Conclusions

Two new palladium coordination-based organic multilayers were assembled using a two-step layer-by-layer scheme. Both colloidal palladium and $PdCl_2(PhCN)_2$ gave organized multilayers with a linear increase in the average chromophore density for each additional molecular layer. The wettability is almost identical for both films, though the roughness and film thickness were an order of magnitude lower for the $PdCl_2$-based system. The optical properties of the two films differ by an order of magnitude both in terms of UV−vis absorption increase and also with respect to shift in absorption maximum. It is clear that the metal complex precursor controls both the optical and the structural properties of the organic layers. The $PdCl_2$-based system exhibited an overall shift in λ_{max} of 23 nm in the multilayer assembled on the template layer, indicating significant electronic communication in the system. No such shift was observed for the colloid-based system. The orientation of the entire $PdCl_2$-based multilayer assembly is determined by the

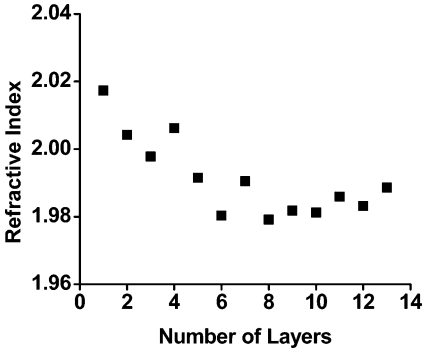

Figure 7. Real part of refractive index at $\lambda = 633$ nm versus number of layers for $PdCl_2$-based multilayers as determined by spectroscopic ellipsometry, fitting the three-term Cauchy equation to the XRR-determined film thickness.

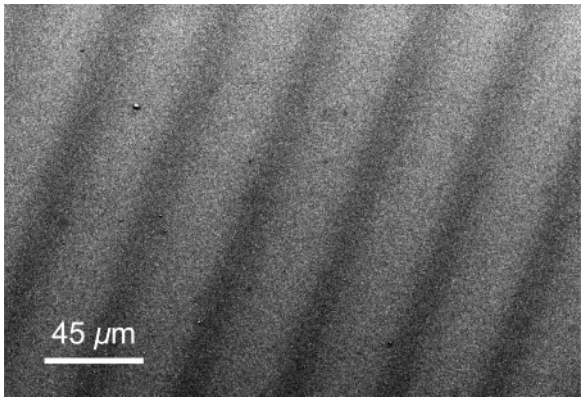

Figure 8. Representative SEM image of a bottom-up patterned colloid-based film with a nominal 5 μm line width and 40 μm pitch formed by the bottom-up approach.

~110° angle of the alkyl-C bonds of the template layer. Subsequent layers retain this orientation, and the film grows at an angle of ~20°, relative to the plane. This is a clear example that structural features of a monolayer interface can be retained and enhanced over distances ranging into the submicron domain using late transition-metal-based coordination chemistry. This ability could permit the a priori design of multilayer properties, including optical absorption, intermolecular coupling, and chemical functionality, by selecting the appropriate molecule for template layer formation. Palladium-colloid-based multilayers were formed successfully on both pyridyl- and hydroxyl-terminated template layers with no apparent differences in the average number of chromophores adsorbed in each bilayer, chromophore orientation, and/or chromophore−chromophore interaction. Interestingly, bottom-up formation of multilayer assemblies was achieved using photopatterned templates patterned with lines with a pitch of 40 μm. By varying the chromophore and metal complex components of the system, this two-step deposition scheme could be used to assemble stable custom-designed 3D multilayer materials, including hybrid or mixed films.

Experimental Section

Compound **1** and $PdCl_2(PhCN)_2$ were prepared according to a published procedure.[94,95] Reagents were purchased from Aldrich or Merck and used as received. Solvents were reagent grade (AR) from either Bio-Lab (Jerusalem) or Frutarom (Haifa). Tetrahydrofuran (THF) was distilled under Ar over Na and degassed before introduction into an M. Braun glovebox. Acetone was dried under N_2 and degassed before introduction into the glovebox. Single-crystal silicon ⟨100⟩ substrates, purchased from Wafernet (San Jose, CA) and ITO (Aldrich), were cleaned by sonication in acetone followed by ethanol and dried under an N_2 stream. Subsequently, they were cleaned for 20 min with UV and ozone in a UVOCS cleaning system (Montgomery, PA). Glass slides (Chase Scientific Glass, Rockwood TN) were cleaned by immersion in a hot (70°C) "piranha" solution (7:3 (v/v) H_2SO_4/30% H_2O_2) for 1 h. Caution: piranha solution is an extremely dangerous oxidizing agent and should be handled with care using appropriate personal protection. The substrates were then rinsed with deionized water followed by the RCA cleaning protocol: 1:5:1 (v/v) $NH_3{\cdot}H_2O$/H_2O/30% H_2O_2 at room temperature for 45 min.[76] The substrates were subsequently washed with deionized water and dried under an N_2 stream and then in an oven for 2 h at 130 °C. Template layer formation was carried out under an inert atmosphere using standard Schlenk/cannula techniques. Advancing contact angles (CAs) were measured on a Ramé-Hart (Netcong, NJ) model 100-00 goniometer. UV−vis spectra were recorded with a Cary 100 spectrophotometer. Scanning electron micrographs were recorded with an in-line secondary electron detector on a SUPRA 55VP FEG LEO microscope. Atomic force microscopy (AFM) images were recorded using a Solver P47 (NT-MDT, Russia) operated in the semicontact mode. The cantilevers used were a W_2C coated CSC12 series of ultrasharp silicon (MikroMash, Estonia) with a resonant frequency of 60−100 kHz and a tip radius of ~10 nm. Roughness data (R_{rms}) were extracted from 500 nm × 500 nm images. X-ray reflectivity (XRR) measurements were carried out with $\lambda = 1.24$ Å at Beamline X23B of the National Synchrotron Light Source (Brookhaven National Laboratory). Details and the data acquisition and analysis procedures are given elsewhere.[82] Refractive indices were estimated using a J. A. Woollam (Lincoln, NB) model M-2000V variable angle spectroscopic ellipsometer with VASE32 software. Measurements were performed on silicon at 65°, 70°, and 75° over a range of 399−1000 nm. The A, B, and C parameters were fit iteratively, with MSE < 10, to a Cauchy model, using the film thickness determined by XRR. The ^{1}H NMR and $^{13}C\{^1H\}$ spectra were recorded at 250.17 MHz on a Bruker DPX 250 and 100.6 MHz on a Bruker AMX 400 NMR spectrometer, respectively. All chemical shifts (δ) are reported in ppm, and coupling constants (J) are in Hz. The ^{1}H and $^{13}C\{^1H\}$ NMR chemical shifts are relative to tetramethylsilane; the resonances of the residual protons of the solvent were used as an internal standard for ^{1}H and all-*d* solvent peaks for $^{13}C\{^1H\}$. All measurements were carried out at 298 K.

Formation of Chromophore 2. An 8-fold excess of 3-iodo-*n*-propyl-1-trimethoxysilane (0.741 g, 2.56 mmol) was added to a dry THF solution (20 mL) of chromophore **1** (0.060 g, 0.331 mmol) under N_2 in a glass pressure vessel.[74] The reaction mixture was stirred and heated for 48 h at 77 °C. Subsequently, the volume was reduced by evaporation under vacuum at room temperature to ~3 mL. Addition of dry pentane (10 mL) to the reaction mixture at −25 °C resulted in the precipitation of **2**. The precipitate was isolated by filtration, washed repeatedly with cold, dry pentane, and dried under a high vacuum yielding chromophore **2** (yield >90%). ^{1}H NMR (250 MHz, $CDCl_3$) δ 8.87 (d, $^3J = 6.5$ Hz, 2H; pyr), 8.44 (d, $^3J = 6.3$ Hz, 2H; pyr), 7.90 (d, $^3J = 6.5$ Hz, 2H; pyr), 7.58 (d, $^3J = 16.0$ Hz, 2H; CH═CH), 7.48 (d, $^3J = 8.0$ Hz, 2H; pyr), 7.42 (d, $^3J = 8.0$ Hz, 2H; ArH), 7.22 (m, 2H; ArH), 7.09 (d, $^3J = 10.0$ Hz, 2H; ArH), 6.95 (d, $^3J = 16.0$ Hz, 2H; CH═CH), 4.59 (t, $^3J = 8.0$ Hz, 2H; N−CH_2), 3.43 (s, 9H; $Si(OCH_3)_3$), 2.0 (m, 2H; CH_2), 0.53 (t, $^3J = 8.0$ Hz, 2H; CH_2Si). $^{13}C\{^1H\}$ NMR (100 MHz, DMSO-d_6) δ 6.02 (CH_2Si), 25.03 (CH_2), 50.79 ($Si(OCH_3)_3$), 67.6 (N−CH_2), 121.59−153.34 (20C, Aromatic and ethenyl carbons). UV−vis (acetone) λ/nm, ($\epsilon \times 10^{-4}$/cm^{-1} M^{-1}) 381 (4.1).

Template Layer Formation. Under N_2, freshly cleaned glass, ITO, and silicon substrates were loaded into a Teflon sample holder,

(94) Burdeniuk, J.; Milstein, D. *J. Organomet. Chem.* **1993**, *451*, 213−220.
(95) Anderson, G. K.; Lin, M. *Inorg. Synth.* **1990**, *28*, 60−63.

immersed in a dry THF solution (0.4 mM), and heated at 77 °C for 16 h in a sealed pressure vessel with the exclusion of light. The functionalized substrates were then rinsed repeatedly with THF and sonicated twice in THF followed by acetone and ethanol sonication for 6 min each. The substrates were dried under a stream of N_2. The assembly process was carried out in a single reaction vessel using standard cannula techniques to transfer the solutions.

Formation of Pd-Colloid-Based Multilayer. Template layer functionalized glass, ITO, and silicon substrates were loaded onto a Teflon holder and immersed for 30 min, at room temperature, in 0.3 mM K_2PdCl_4 in DI water (Barnstead, ~1 μS/cm) which was mixed for 1 min prior to immersion. The samples were then rinsed in DI water and dried under a stream of N_2. Subsequently, the samples were immersed for 30 min in a 1 mM solution of chromophore **1** in THF at room temperature. The solution was stirred for at least 15 min before immersion. The samples were then sonicated twice in THF and once in acetone for 5 min each. They were then rinsed with ethanol and dried under an N_2 stream. These steps were repeated 6 times each, each time in a freshly prepared solution. No attempts have been made to control the properties/structure of the palladium interlayers, for instance, by controlling the pH and/or the ionic strength.[96]

Formation of $PdCl_2$-Based Multilayer. Cleaned glass and silicon substrates were loaded onto a Teflon holder and immersed for 15 min, at room temperature, in a 1 mM solution of $PdCl_2(PhCN)_2$ in THF. The samples were then sonicated twice in THF and once in acetone for 3 min each. Subsequently, the samples were dipped in THF and immersed for 15 min in a 1 mM solution of compound **1** in THF at room temperature. The solution was stirred for at least 15 min before immersion. The samples were then sonicated twice in THF and once in acetone for 5 min each. This procedure was repeated 6 times. Finally, samples were rinsed in ethanol and dried under a stream of N_2.

(96) Brinker, C. J.; Sherer, G. W. *Sol−Gel Science: The Physics and Chemistry of Sol−Gel Processing*; Academic Press: San Diego, CA, 1990

Multilayer Assembly on Patterned Template Layer. Fully deprotected and photopatterned trimethoxy-[11-(2-nitro-benzyloxy)-undecyl]-silane films[93] were used as a template layer for the formation of Pd-colloid-based multilayers. Immersion of the substrates in 0.3 mM K_2PdCl_4 in DI water was followed by immersion in compound **1**, as described above. This procedure was repeated 4 times in ambient conditions. The UV−vis absorption was recorded, as for the previous films, for the monolayer and for the unpatterned films after deposition of each additional layer. The patterned films with the deposited multilayer were imaged by scanning electron microscopy (SEM).

Acknowledgment. Research was supported by the Robert Rees Fund for Applied Research, the Bikura foundation of The Israel Academy of Sciences and Humanities, BMBF, and the MJRG for Molecular Materials and Interface Design. X-ray reflectivity measurements were performed at Beamline X23B of the National Synchrotron Light Source, which is supported by the U.S. Department of Energy. We thank Dr. H. Cohen for XPS measurements, Dr. R. Bar-Ziv and his group for their help with the photodeprotection, and Prof. R. Naaman for fruitful discussions (all WIS). We also thank Mr. D. Strawser (WIS) and Prof. H.-B. Kraatz (University of Saskatchewan) for preliminary experiments and Dr. D. Freeman (WIS) for her skillful synthetic contribution. M.E.vd.B. is the incumbent of the Dewey David Stone and Harry Levine career development chair.

Supporting Information Available: Semicontact AFM image of template layer of **2** on silicon (Figure S1) and spectroscopic ellipsometry data Ψ and Δ for the $PdCl_2$-based multilayer (Figure S2). This material is available free of charge via the Internet at http://pubs.acs.org.

JA061026E